ACS APPLIED MATERIALS & INTERFACES

Research Article

Cite This: ACS Appl. Mater. Interfaces XXXX, XXX, XXX−XXX

www.acsami.org

Stretchable Seal

Paul Le Floch,[†,∥] Shi Meixuanzi,[‡,∥] Jingda Tang,[‡] Junjie Liu,[†,§] and Zhigang Suo*[,†]

[†]School of Engineering and Applied Sciences, Kavli Institute for Bionano Science and Technology, Harvard University, Cambridge, Massachusetts 02138, United States

[‡]State Key Lab for Strength and Vibration of Mechanical Structures, Department of Engineering Mechanics, Xi'an Jiaotong University, Xi'an 710049, China

[§]State Key Laboratory of Fluid Power and Mechatronic System, Key Laboratory of Soft Machines and Smart Devices of Zhejiang Province, and Department of Engineering Mechanics, Zhejiang University, Hangzhou 310027, China

Supporting Information

ABSTRACT: Many stretchable electronic devices require stretchable hermetic seals. However, stretchability and permeability are inextricably linked at the molecular level: stretchable, low-permeability materials do not exist. We collect data for the permeation of water and oxygen in many materials and describe the scaling relations for both flat and wrinkled seals. Whereas flat seals struggle to fulfill the simultaneous requirements of stretchability, low stiffness, and low transmissibility, wrinkled seals can fulfill them readily. We further explore the behavior of wrinkled seals under cyclic stretch using aluminum, polyethylene, and silica films on elastomer substrates. The wrinkled aluminum develops fatigue cracks after a small number of cycles, but the wrinkled polyethylene and silica maintain low transmissibility after 10 000 cycles of tensile strain.

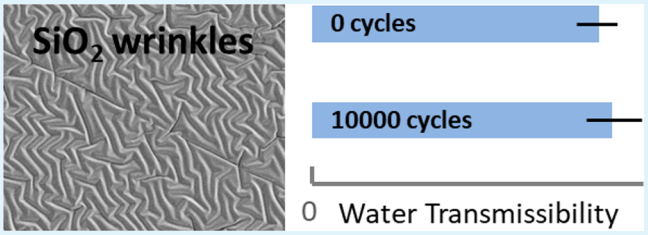

KEYWORDS: *hermetic seal, stretchable electronics, permeability, wrinkles, laminates*

INTRODUCTION

Hermetic seals are ubiquitous. Plastics and metals seal food and drug,[1] oxides and nitrides seal microelectronics,[2,3] and butyl rubber seals tires.[4] Except for the last example, seals in general are made of stiff materials: plastics, metals, and ceramics. The recent decade has seen the emergence of stretchable electronics,[5−10] soft robots,[11−13] hydrogel ionotronics,[14] and soft medical devices.[15,16] For long-time use, these devices will also require seals. Without hermetic seals, silver nanowires, copper nanowires, and liquid metals oxidize,[17−19] conducting polymers degrade[20,21] and hydrogels dehydrate.[22] In an island-bridge design of stretchable electronics, nonstretchable electronic materials are placed on stiff islands, which are attached to a soft substrate and are bridged by stretchable interconnects.[23] A stretchable interconnect can be made of a stiff material by the means of unidirectional buckles[24−26] or flat serpentines.[27,28] Stiff materials can seal the islands, as well as the buckled and serpentine interconnects, just like a coiled phone cord, which is electrically insulated by a thin layer of plastic. It has been a challenge, however, to seal intrinsically stretchable materials.[29−35] Stretchable functional materials with long-term reliability in ambient conditions may be developed, such as crumpled graphene,[17,36] but this strategy would push the development of soft devices into a narrow path, excluding many materials of superior electronic properties and well-established processing methods. In general, electronic functions and hermetic seals require different materials.

The search for stretchable seals has highlighted a fundamental fact of nature: stretchable and low-permeability materials do not exist.[22] At the molecular level, stretchability and permeability are inextricably linked. Stretchability comes from the entropic elasticity of polymer chains. In an elastomer, the polymer chains are cross-linked to form a three-dimensional network. To be stretchable, each individual polymer chain contains hundreds or more monomer units and undergoes ceaseless thermal motion. Consequently, small molecules, such as water and oxygen, diffuse in an elastomer as readily as in a polymer liquid. The permeability of small molecules in an elastomer is insensitive to cross-link density and applied stretching. An elastomer is solid-like at the scale above the mesh size of the network, but liquid-like at the scale below.

Here, we propose to break the stretchability−permeability trade-off by demonstrating stretchable seals using wrinkled films of stiff materials. We collect data on the permeability of water and oxygen for various materials and confirm that no stretchable materials has low enough permeability to serve as hermetic seals for electronics. We develop a scaling model to show that thin and wrinkled films of many stiff materials have both high stretchability and low permeability to serve as stretchable seals. Unlike electrical interconnects made of stiff materials, hermetic seals require two-dimensional, continuous films. To

Received: May 29, 2018
Accepted: July 17, 2018
Published: July 17, 2018

DOI: 10.1021/acsami.8b08910
ACS Appl. Mater. Interfaces XXXX, XXX, XXX−XXX

make it stretchable in any in-plane direction, two-dimensional wrinkles are needed. Two-dimensional wrinkles do not affect the permeability of the seal initially, but may develop large local deformation, so that repeated stretch may cause fatigue cracks. To explore these fundamental considerations, we study wrinkled aluminum, polyethylene, and silica films on elastomer substrates. We show that the wrinkled aluminum film develops fatigue cracks after a small number of cycles, but the wrinkled polyethylene and silica films maintain low transmissibility after 10 000 cycles of tensile strain.

PERMEABILITY OF MATERIALS AND COMPOSITE STRUCTURES

The transmissibility T of a gas through a solid film is defined by[37]

$$T = \frac{P}{h} = \frac{J}{\Delta\Pi} \tag{1}$$

where h (m) is the thickness of the film, P ($m^2/s/Pa$) is the permeability, $\Delta\Pi$ (Pa) is the difference in the partial pressures of the gas on the two sides of the film, and J is the flux of molecules of the gas through the film ($m^3/m^2/s$).

We plot various materials in the space of water permeability and elastic modulus, as well as in the space of oxygen permeability and elastic modulus (Figure 1). The data correspond to the measurement carried out at ambient pressure and in the temperature range 23−40 °C.

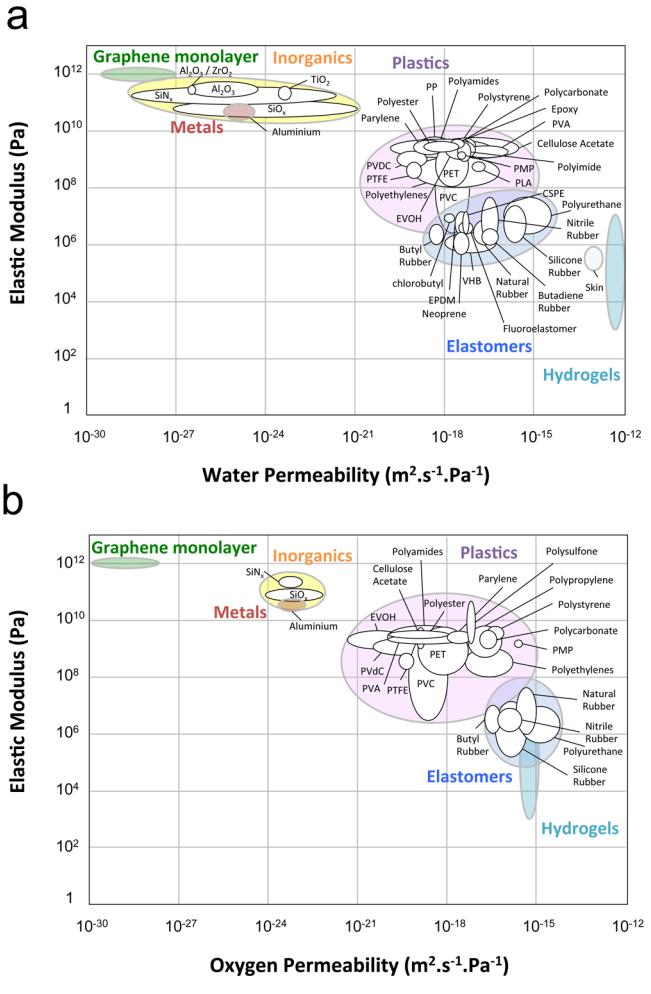

Figure 1. Soft and low-permeability materials do not exist. Materials are plotted in (a) the space of water permeability and elastic modulus and (b) the space of oxygen permeability and elastic modulus.

We show in the Supporting Information that the thermal activation of permeability is negligible within this range of temperature compared to the scattering in the data gathered for each material. Also see the Supporting Information for sources of data and notes on their methods of determination (Table S1).[22,38−98] This is perhaps the first time that such a broad range of materials are compared in the permeability−modulus space. The data gathered for each individual material scatter significantly. The permeability of an elastomer or a plastic scatters over 1−2 orders of magnitude. The permeability of an inorganic material, such as silica and silicon nitride, scatters even more. This scattering results from two factors. First, the permeability depends on the microstructures of the materials. For instance, defects in vitreous silica can affect its permeability.[99−101] Second, permeability is measured under different conditions, such as different temperature or gas pressure (Table S1).

For all the materials gathered here, modulus spans over 10 orders of magnitude, and permeability spans over 15 orders of magnitude. A graphene monolayer has an elastic modulus of 1 TPa and a water permeability lower than 10^{-27} $m^2/s/Pa$. For conventional electronic packaging,[2] the inorganic materials, such as silicon dioxide and silicon nitride, are used. These passivation layers suffer from pinholes and cracks. Organic sealants like epoxies, polyimide, and polyxylene (Parylene) are sometimes used instead. For flexible electronics like organic light-emitting diode (OLED) displays, flexibility of the seal is an additional constraint, and polymer−inorganic multilayered architectures have been developed.[3] Elastomers and hydrogels have low elastic modulus but high permeability. The large white holes in both spaces affirm the fundamental fact of nature: soft and low-permeability materials do not exist.

Of all the materials, only elastomers are capable of large and elastic stretch. Among elastomers, the butyl rubber is the least permeable, but its permeability for water and oxygen is more than 10 000 times that of silicon dioxide (Figure 1).[22,47−51,87,102] Butyl rubber has been proposed to seal flexible and stretchable electronics,[102,103] but its efficacy is uncertain. The information on water and oxygen sensitivity for stretchable electronic materials is scanty and mostly qualitative. In microelectronics, it is common practice to seal devices with a silicon dioxide layer of at least 100 nm. According to eq 1, however, 1 mm of butyl rubber must be used to reach the same level of transmissibility. As another example, to last more than 10 000 h, OLEDs and organic solar cells[3,98,104,105] require a water vapor transmission rate (WVTR) lower than 10^{-6} $g/m^2/day$ (i.e., a transmissibility of 8×10^{-21} $m/s/Pa$) and an oxygen transmission rate (OTR) lower than 10^{-5} $mL/m^2/day$ (i.e., a transmissibility of 6×10^{-21} $m/s/Pa$), assuming that the relative humidity difference is 50% and that the oxygen partial pressure is 21 kPa in the ambient atmosphere. A thickness of 0.5−5 mm would be required to satisfy the WVTR criteria and a thickness of about 10 cm is required to satisfy the OTR criteria. Again, a butyl rubber seal would be even thicker than submillimeter devices.

Composites have long been used as seals in the food packaging industry, as well as the OLED coating industry. A stiff, low-permeability material (e.g., an oxide, a nitride, or graphene) is integrated as barriers in a matrix (e.g., a plastic or an elastomer).[106−108] The barrier material can be used as a continuous layer, or as nanoparticles with a large aspect ratio. The former is the laminate structure and the latter is the brick−mortar structure. Both structures can lower the permeation of small molecules, but neither can be made soft and stretchable (Figures S1 and S2).

STIFFNESS−TRANSMISSIBILITY TRADE-OFF

For a seal of permeability P and thickness h, the transmissibility is $T = P/h$. When a flat film is stretched, the stiffness is Eh, where E is the elastic modulus. When a wrinkled film is stretched, the stiffness scales as Eh^3/L^2, where L is the period of the wrinkles. The trade-off between stiffness and transmissibility is different for a flat and a wrinkled seal. These relations and their implications for stretchable seals are discussed in this section.

DOI: 10.1021/acsami.8b08910
ACS Appl. Mater. Interfaces XXXX, XXX, XXX−XXX

For numerical illustration, we will use water permeability for various materials.

Stiffness of a Flat Seal. Consider a flat seal under uniaxial tension (Figure 2). The force F is proportional to the tensile strain $\delta l/l$

$$\frac{F}{w} = Eh\frac{\delta l}{l} \tag{2}$$

where w is the width of the film and Eh is the stiffness. We plot each material as a parallelogram in the space of stiffness and transmissibility (Figure 2). The top edge of a parallelogram corresponds to the stiffness of a material of a thickness of 1 mm, and the bottom edge corresponds to a thickness of 10 nm. The horizontal width of the parallelogram corresponds to the scatter in the permeability of the material (Table S1). As a numerical illustration, we draw a vertical line corresponding to the required limit of transmissibility for OLEDs mentioned previously.[3] The seal needs to limit the transmissibility to the left of the vertical line. All plastics and elastomers are too permeable to fulfill the requirement. All the stiff seals can be used to protect flexible electronics provided the strain of the devices is sufficiently small to avoid breaking.[109] Graphene and ultrathin films of oxides and nitrides may sustain a few percent of tensile strain.[81,110,111] They may potentially be used to seal devices of small stretchability. We draw a horizontal line corresponding to a soft device of a modulus of 1 MPa and a thickness of 1 mm, which gives a stiffness of 10^3 N/m. We stipulate that the stiffness of the seal should not exceed that of the device, which limits the stiffness of the seal below the horizontal line. The lower left quadrant of the stiffness−transmissibility is empty. A 100 nm thick silica seal is too stiff, but stays within the required limit of transmissibility. According to the lowest value of transmissibility reported in the literature,[80] a graphene monolayer (0.335 nm thick, indicated by the horizontal green segment in Figure 2) is compliant enough, and approximately fulfills the transmissibility criteria.

In Figure 2, we have drawn the vertical and horizontal lines under certain assumptions. Under different assumptions, the two lines will move, and the lower left quadrant may contain some candidates. However, it will be a challenge for flat seals to have both low stiffness and low transmissibility.

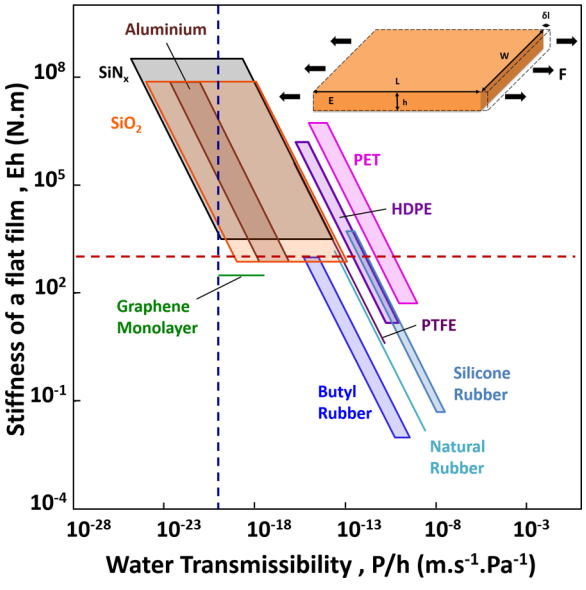

Figure 2. Stiffness−transmissibility diagram for flat seals. Each material is represented by a parallelogram, where the water permeability varies between a maximum and a minimum value (according to Table S1) and the thickness h varies between 1 mm and 10 nm.

Stiffness of a Wrinkled Seal. We consider now a seal with a wavy shape in one direction, attached to a substrate (i.e., a soft device) at the troughs of the wave (Figure 3). When an in-plane force F is applied, the seal will be deformed between each attachment point. For an inextensible thin film, the deformation is pure bending. By analogy with the buckling of an elastica,[112−116] we derived that the force F needed to compress a wrinkled film is (Supporting Information)

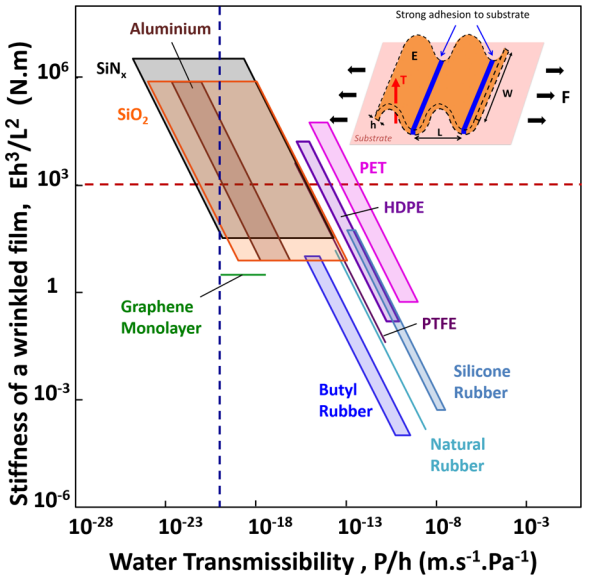

Figure 3. Stiffness−transmissibility diagram for wrinkled seals. Each material is represented by a parallelogram, where the water permeability varies between a maximum and a minimum value (according to Table S1) and the thickness h varies between 1 mm and 10 nm. For the stiffness of the wrinkled film, we set $h/L = 0.1$. Thin films of low-permeability materials (e.g., graphene, silica, silicon nitride) give sufficiently low stiffness and low transmissibility.

$$\frac{F - F_b}{w} = \frac{5.56}{12(1-\nu)}\frac{Eh^3}{L^2}\frac{\delta L}{L} \tag{3}$$

where F_b is the force required to initially buckle the film between two attachment points, w and h are, respectively, the width and the thickness of the film, ν is the Poisson's ratio, E is the elastic modulus of the material, and L is the period of the wrinkles. $\delta L/L$ is the relative change in the wrinkles period. The numerical prefactor $\frac{5.56}{12(1-\nu)}$ is close to 1. Eq 3 is a linear interpolation for $\delta L/L$ in the range $[0; 0.2]$. This approach shows that the rigidity Eh^3/L^2 is the parameter of interest to describe the stiffness of a wrinkled thin film. This conclusion can also be reached using dimensional analysis (Supporting Information). The wrinkles stiffness is lower than the stiffness of the flat film by a factor h^2/L^2 and allows large stretchability of the film.

For a wrinkled film, the thickness h is much smaller than the wavelength L. For numerical illustration, we set $h/L = 0.1$, so that $Eh^3/L^2 = 0.01Eh$. We plot each material as a parallelogram in the space of transmissibility and stiffness of a wrinkled film (Figure 3). In this case, the lower left quadrant contains the commonly used sealing materials. A 100 nm thick wrinkled silica seal will fulfill both transmissibility and stiffness requirements.

DOI: 10.1021/acsami.8b08910
ACS Appl. Mater. Interfaces XXXX, XXX, XXX−XXX

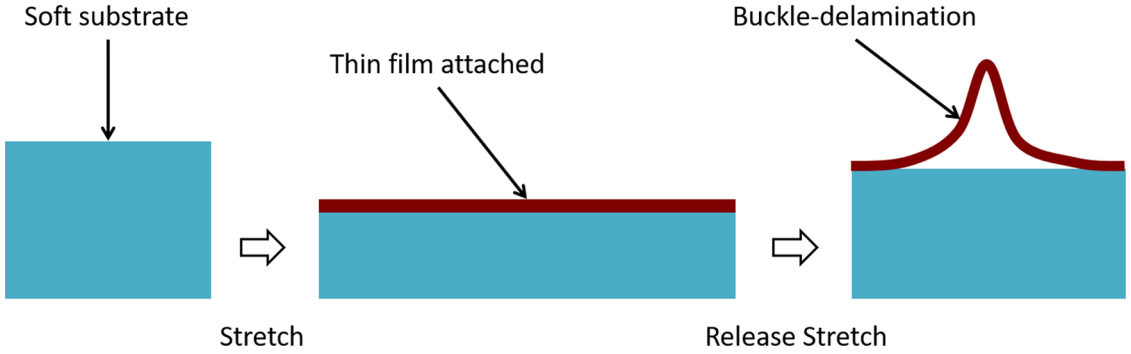

Figure 4. Substrate is prestretched and a thin film of low-permeability material is attached to it. When the prestretch is released, the film undergoes buckle delamination.

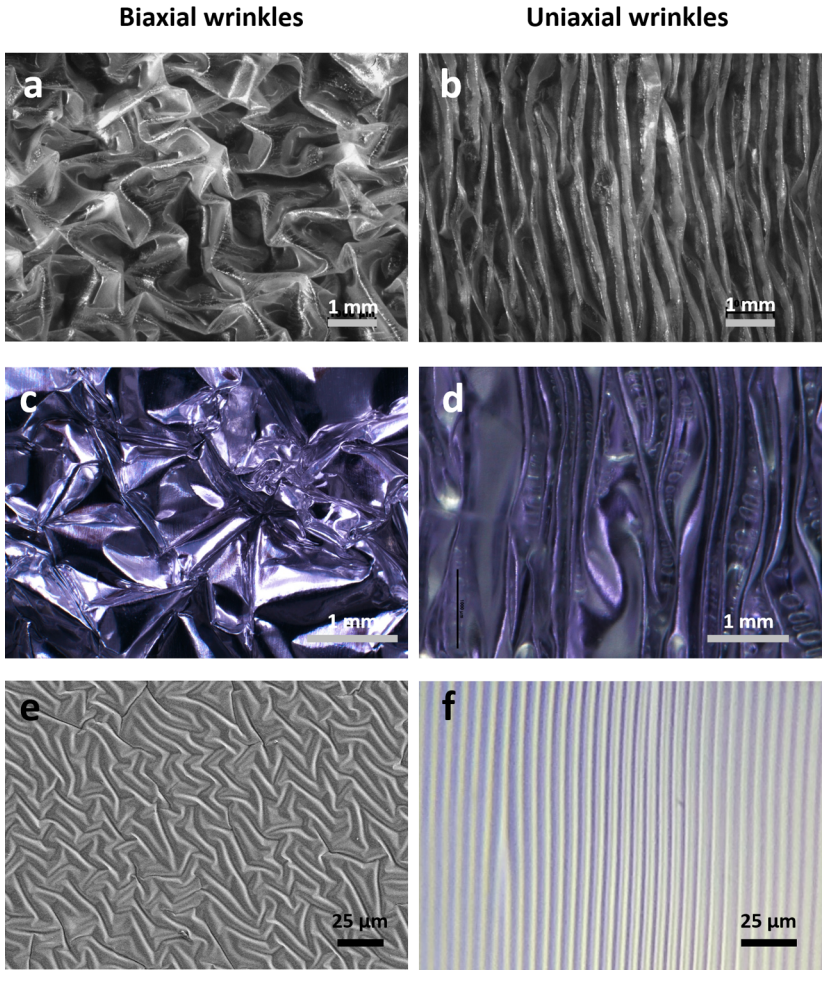

Figure 5. Biaxial and uniaxial wrinkles of various stiff materials on soft substrates. (a) Polyethyelene (27 μm) on a biaxially prestretched (2.5 × 2.5 times) VHB (500 μm). After release, the residual biaxial stretch is 1.75 × 1.75. (b) Polyethylene on a uniaxially prestretched VHB (4 times). After release, the residual uniaxial stretch is 1.67. For (a) and (b), scale bars are 1 mm. (c) Biaxially prestretched (4 × 4 times) VHB (1 mm)/aluminum (26.5 μm)/VHB (1 mm). Scale bar = 5 mm. (d) Uniaxially prestretched (5 times) VHB (2 mm)/aluminum (26.5 μm)/VHB (2 mm). Scale bar = 1 mm. (e) Silica (50 nm) on a biaxially prestretched (1.23 × 1.23 times) PDMS substrate (200 μm). (f) Silica (50 nm) on a uniaxially prestretched (1.20 times) PDMS substrate (200 μm). For (e) and (f), scale bars are 25 μm. The residual stretch is negligible for silica wrinkles on PDMS.

Furthermore, the relative change in the wrinkles period, $\delta L/L$, can be large, even though the local deformation is small. As another example, a 100 μm thick poly(tetrafluoroethylene) can be used to achieve the desired stiffness, but with a transmissibility as low as 10^{-16} m/s/Pa. Here, we only considered the case where $h/L = 0.1$, but wrinkles with a larger wavelength could be designed to achieve lower levels of stiffness.

USING WRINKLES TO MAKE SOFT, LOW-PERMEABILITY SEALS

To illustrate the previous analysis, we prepared wrinkled seals using buckle-delamination[117,118] of a thin, stiff and low-permeability material on a soft substrate (Figure 4). Uniaxial and biaxial wrinkles were studied. The amount of delamination depends on the substrate/film adhesion, which we did not

DOI: 10.1021/acsami.8b08910
ACS Appl. Mater. Interfaces XXXX, XXX, XXX−XXX

investigate here. When a film is bent, the strain is given by $\varepsilon = y/R$, where R is the radius of curvature and y is the distance of the material particle in the film from the neutral surface. Using $y \sim h$ and $R \sim L$, we estimate $\varepsilon \sim h/L$. The failure strain is on the order of 1% for stiff materials. These elementary considerations suggest that one should be careful in designing a wrinkled film to avoid rupture. Furthermore, two-dimensional wrinkles may develop localized large deformation. It is difficult to quantify the failure conditions analytically. We use uniaxial tension to study experimentally the stress−stretch behavior and the fatigue of wrinkled seals.

We studied three film/substrate systems. The first two systems used an acrylic elastomer VHB as the substrate and a polyethylene and an aluminum foil as the films. As discussed above, polyethylene and aluminum are too permeable to seal air-sensitive devices, but these materials are readily available and easily handled. Here, we used them to explore the behavior of wrinkled seals under cyclic stretch. The third system involves silica films deposited on a poly(dimethylsiloxane) (PDMS) substrate.

For the polyethylene/VHB system, the VHB layer was 500 ± 10 μm thick and the polyethylene film was 27 ± 2 μm thick. We applied both uniaxial and biaxial stretches to the VHB elastomer before attaching polyethylene films. Then, the prestretch is released and the thin films wrinkle. Figure 5a shows optical micrographs of polyethylene thin film (Glad Press'N Seal food wrap) on a sheet of biaxially prestretched VHB (biaxial stretch = 2.5 × 2.5 times). The prestretch is then released in both directions simultaneously. After release, the residual stretch is 1.75 × 1.75. We can clearly see the wrinkles and the delamination in the polyethylene films. The wrinkles have some common features with the herringbone patterns, but are more random.[119,120] Figure 5b shows a polyethylene thin film on a sheet of uniaxially prestretched VHB (stretch = 4 times). After release, the residual stretch is 1.67.

Similarly, Figure 5c,d shows the optical micrographs of both biaxial and uniaxial aluminum wrinkles sandwiched between two VHB layers. (Two prestretched layers were necessary to induce the buckling instability.) The aluminum layer is 26.5 ± 2.4 μm thick and the VHB layers are 1 or 2 mm thick, depending on the prestretch applied. Delamination is much less pronounced for the VHB/aluminum/VHB laminates, but it tends to become more severe as the prestretch increases.

Furthermore, we deposited silica films onto poly(dimethylsiloxane) (PDMS) by plasma-enhanced chemical vapor deposition (PECVD) (see Materials section for details on the deposition process). Figure 5e,f shows, respectively, the SEM and optical images of biaxial and uniaxial silica wrinkles on PDMS. Silica films between 5 and 50 (±0.2) nm were deposited on a prestretched (up to 1.30 × 1.30 times) PDMS substrate (200 ± 10 μm). The residual stretch is negligible for silica wrinkles on PDMS, and we did not observe delamination.

The presence of a residual stretch in some cases can be qualitatively explained by estimating the stiffness of the substrate (Eh) and the wrinkled thin film (Eh^3/L^2). In case of polyethylene/VHB, the substrate has a stiffness in the order of 9×10^2 N m. The uniaxial wrinkles period is about 250 μm. Thus, the stiffness of the polyethylene film is about 3×10^2 N m. This rough estimation shows that the two stiffnesses are comparable. The wrinkles can thus limit the release of the prestretch. In case of silica/PDMS, the substrate has a stiffness in the order of 10^3 N m. The period of the uniaxial wrinkles is about 6 μm. Thus, the stiffness of the silica film is about 3×10^{-1} N m. The silica wrinkles are much softer than the substrate, which explains why the prestretched is completely released.

Mechanical Properties of the Wrinkled Laminate. As expected, the laminate of a wrinkled film on an elastomer is stretchable. We use uniaxial tension to quantify the stretchability of uniaxially prestretched wrinkled laminates (Figure S5). When the prestretch increases, the amplitude of the wrinkles becomes larger, and their wavelength decreases slightly, which leads to a larger stretchability. In uniaxial tension, if the stretch applied is lower than the initial prestretch, the wrinkled laminate is stretchable, and almost as soft as the substrate. Stretching further will cause delamination of the coating or cracks. Both scenarios lead to failure of the laminate.

We measured the electrical resistance of the aluminum film while subjecting the laminate to cyclic stretch (Figure S6a). After a small number of cycles, the resistance of the aluminum jumps to a very high value (Figure S6b) because cracks have propagated through the width of the sample (Figure S6c,d) and the aluminum film is not continuous anymore. Thus, the VHB/aluminum/VHB laminate is not a good choice for designing stretchable seals. By contrast, the polyethylene/VHB and silica/PDMS systems do not develop cracks under cyclic stretch.

Water Transmissibility of Wrinkled Laminates. We measured the water transmissibility of polyethylene/VHB and silica/PDMS using the dry-cup test.[22] Both laminates have lower water transmissibility than the bare substrates (Figure 6). Wrinkled laminates have a higher water transmissibility than the flat one. It can be explained partially because of the area prestretch and the residual area stretch. Because the elastomer substrate is incompressible, the residual area stretch implies a decrease in thickness (Figure S7), which increases the water transmissibility through the elastomer, according to eq 1. Also, the wrinkled plastic layer has a larger surface than the elastomer substrate (Figure S7). We propose a simple model to consider these effects (Supporting Information) and derive a formula to predict the transmissibility of wrinkled laminates

$$\frac{1}{T_{\text{eff}}} = \frac{1}{\lambda_r}\frac{1}{T_s} + \frac{\lambda_r^2}{\lambda_p}\frac{1}{T_f} \tag{4}$$

The effective transmissibility T_{eff} depends on the transmissibility of the elastomer substrate T_s, the transmissibility of the plastic film T_f, the area prestretch λ_p, and the residual area stretch λ_r. We measured individually the water permeability of VHB and polyethylene while measuring the transmissibility of the laminates (Figure 6a). We obtained $P_{\text{VHB}} = (4.19 \pm 0.58) \times 10^{-17}$ and $P_{\text{PE}} = (1.17 \pm 0.04) \times 10^{-18}$ m^2/s/Pa. These values are in good agreement with our previous measurements for VHB[22] and the literature of polyethylene (Table S1). Similarly, we also measured the water permeability of bare PDMS and silica/PDMS laminates (Figure 6b). We obtained $P_{\text{PDMS}} = (2.42 \pm 0.13) \times 10^{-16}$ m^2/s/Pa, which is also in good agreement with our previous measurement.[22] Because silica was deposited by PECVD, we were not able to measure the permeability through silica alone. We extrapolate its permeability using a flat PDMS/silica laminate and eq 4. For a thickness of 5 nm of silica, we extrapolate $P_{\text{silica}} = (6.77 \pm 0.14) \times 10^{-22}$ m^2/s/Pa. This value is high for bare silica, still in the range of values that we obtained from the literature about silica/plastic laminates (Table S1). We also measured λ_p and λ_r for each sample, which allows us to use eq 4 to predict the effective water transmissibility of wrinkled laminates (Figure 6a,b). For the polyethylene/VHB system, the prediction for the flat laminate is very close to the experimental

DOI: 10.1021/acsami.8b08910
ACS Appl. Mater. Interfaces XXXX, XXX, XXX−XXX

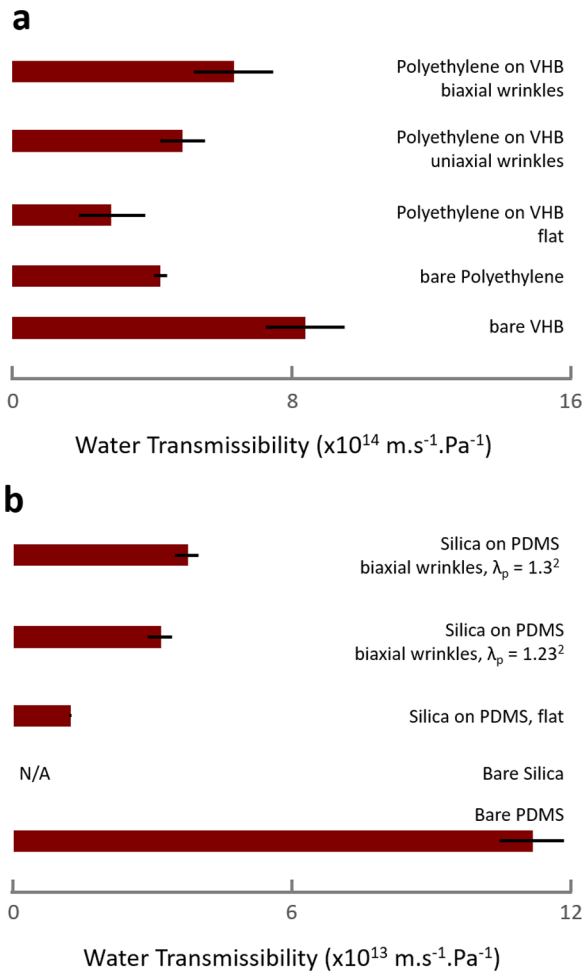

Figure 6. Effective water transmissibility of wrinkled laminates is reduced compared to that of the bare substrate. (a) Polyethylene (27 μm) on VHB (500 μm). The uniaxial prestretch of the VHB substrate is 4 and the residual uniaxial stretch is 1.75. The biaxial prestretch of the VHB substrate is 3.25 × 3.25 and the residual biaxial stretch is 1.75 × 1.75. (b) Silica (5 nm) on PDMS (200 μm). The biaxial prestretch of the PDMS substrate is 1.23 × 1.23 or 1.30 × 1.30. The residual biaxial stretch is negligible in this case.

measurement. For both systems, predictions for wrinkled laminates are significantly lower than the experimental measurements (Figure S8). It may be due to the creation of defects in the thin film during the release of the prestretch, or due to the wrinkles geometry, which is more complex than our model. The absolute error bars on the experimental measurements are one standard deviation. The error bars on the predictions represent the standard uncertainty,[121] which takes both the standard deviations on the transmissibility measurements of the substrate and the film and the typical error on the measurements of the stretches into account (eq S30 in Supporting Information). Our model predicts that the transmissibility increases with the area prestretch. For the polyethylene/VHB system, although the laminate with biaxial wrinkles has a higher transmissibility than the uniaxial and the flat one, it is important to keep in mind that this sample is much thinner because of the effect mentioned above. In terms of effective permeability, it is lower for the laminate with biaxial wrinkles than for the one with uniaxial and flat wrinkles. Furthermore, we noticed that the water transmissibility of laminates does not change over a period of one month.

Fatigue of Transmissibility Properties. We ascertained that the transmissibility of a wrinkled laminate remained low after cyclic loading. We prepared two uniaxially wrinkled laminates under the same experimental conditions. One laminate is a control sample, whereas the other is undergoing a uniaxial tension fatigue test. We repeat this procedure for two biaxially wrinkled laminates. For the polyethylene/VHB system, for the uniaxially wrinkled samples, the uniaxial prestretch is 4 and the residual uniaxial stretch is 1.75. For the biaxially wrinkled samples, the biaxial prestretch is 3.25 × 3.25 and the residual biaxial stretch is 1.75 × 1.75. We first measure the water transmissibility of all the samples simultaneously (Figures 7a and S9a). After a week of testing, we proceed to a first fatigue test (1000 cycles in uniaxial tension). We applied a uniaxial strain of 100% to uniaxially wrinkled samples and a uniaxial strain of 50% to biaxially wrinkled samples during the fatigue test. Then, we measured again the transmissibility of all the samples for another week. We next repeated this procedure for a 10 000-cycle test. There is only a slight increase in the water transmissibility between the control sample and the fatigued one, even after 10 000 cycles (Figures 7a and S9a). The wrinkles morphology is similar after 10 000 cycles (Figures 7b and S9b).

Similarly, we studied the fatigue of transmissibility properties of silica/PDMS wrinkled laminates using the above procedure. The uniaxial strain applied are, respectively, 10 and 20% for biaxially wrinkled laminates with λ_p = 1.23 × 1.23 and 1.30 × 1.30. The water transmissibility remained almost constant with the number of cycles (Figures 7c and S9d). The buckling pattern becomes anisotropic after 10 000 cycles of uniaxial tension (Figure 7d): two preferred orientations are observed, short-range wrinkles parallel to the stretching direction and large-range creases perpendicular to the stretching direction. We hypothesize a mechanism of the formation for this new microstructure: the initial wrinkled laminate is isotropic and the wrinkles orientation continuously varies from perpendicular to parallel to the stretching direction. When a uniaxial strain is applied, wrinkles that are to some degree perpendicular to the stretching direction will flatten more than the ones that tend to be parallelly oriented to the stretching direction. Thus, when the laminate is fully strained in one direction, the remaining wrinkles are mostly parallel to the stretching direction. When the stretch is released, the system is already frustrated by the wrinkles parallel to the stretching direction, which prevents the immediate growth of perpendicular wrinkles. However, further releasing the stretch causes the laminate to undergo more violent modes of buckling, such as creasing. Creases perpendicular to the stretching direction are formed and overlap on the parallel wrinkles (Figure S10). Despite this change in morphology, we do not observe the formation of cracks and additional defects compared to the pristine wrinkled sample, and we measure a steady water transmissibility with the number of cycles.

DISCUSSION

If the laminate undergoes a purely elastic deformation under cyclic stretch, the transmissibility should remain unchanged. But plastic deformations of the thin film can happen, as we observed for wrinkled aluminum. Transmissibility of wrinkled polyethylene films and wrinkled silica can sustain more than 10 000 cycles of large deformation in uniaxial tension. The stress–stretch curves before and after 10 000 cycles are almost identical for the uniaxially wrinkled polyethylene/VHB laminate (Figure S11a). We observed some stiffening for the biaxially wrinkled laminate (Figure S11b). We attribute this effect to the

DOI: 10.1021/acsami.8b08910
ACS Appl. Mater. Interfaces XXXX, XXX, XXX−XXX

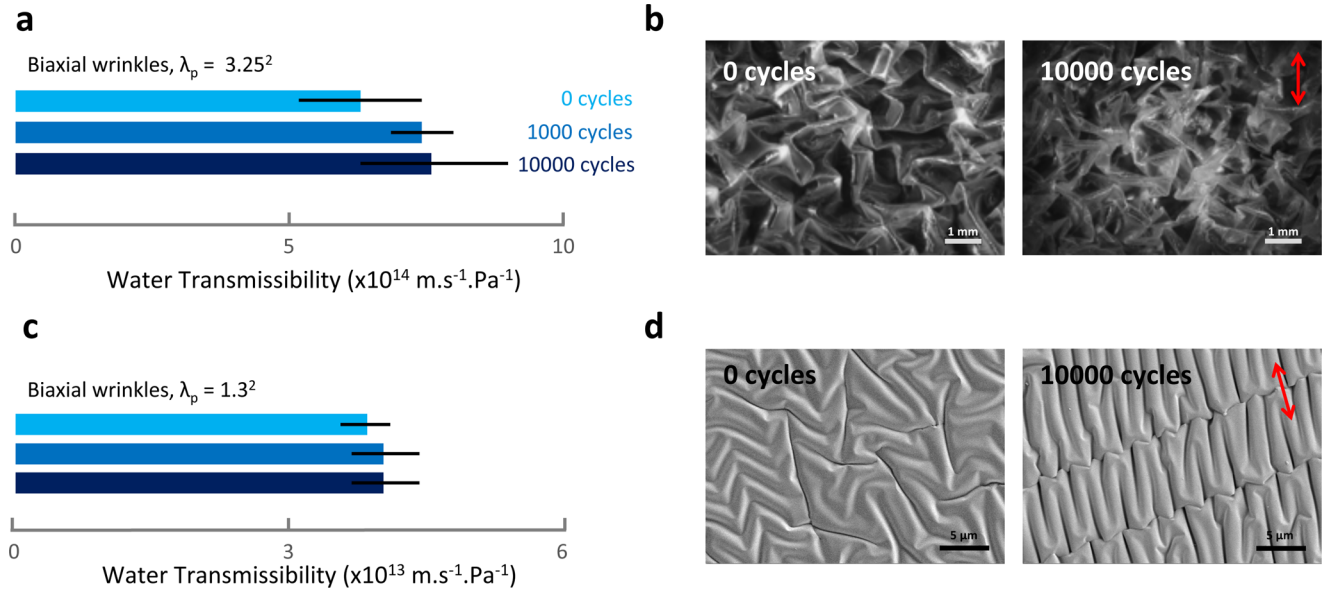

Figure 7. Transmissibility of polyethylene/VHB and silica/PDMS biaxially wrinkled laminates remains low after 10 000 cycles of uniaxial tension. (a) The water transmissibility of polyethylene (27 μm)/VHB (500 μm) biaxially wrinkled laminate (λ_p = 3.25 × 3.25) only increases slightly with the number of cycles. The uniaxial strain applied during the fatigue test is 50%. (b) The morphology of the plastic wrinkles is not changed after 10 000 cycles. The red arrow is the direction of the strain and the scale bars are 1 mm. (c) The water transmissibility of silica (5 nm)/PDMS (200 μm) biaxially wrinkled laminate (λ_p = 1.30 × 1.30) only increases slightly with the number of cycles. The uniaxial strain applied during the fatigue test is 20%. (d) Biaxial silica wrinkles are anisotropic after 10 000 cycles of uniaxial tension. The red arrow is the direction of the strain and the scale bars are 5 μm.

orientation of some wrinkles on the sides of the samples, parallel to the sides of the sample and the stretching direction. These wrinkles cannot be as stretchable as the ones oriented perpendicularly to the stretch direction. Thus, the plastic stiffens the composite if the stretch is too large. Again, this effect was observed principally on the sides of each sample, and may be caused by the edge effects during sample preparation.

In our experiment, the wrinkles morphology is not controlled, although many different patterns have been observed.[122−124] The wrinkles morphology may affect the stress concentration in the thin film, hence, the damage accumulation. It is crucial to understand stress concentration in such structures because seals require continuous, defect-free films. Ordered wrinkles, such as wrinkles with herringbone patterns, lower the elastic energy,[122,125] but it is not clear if this structure also minimizes the stress concentration.

Residual stress in the stretchable seal can also have some aging effects without further stretching. Our transmissibility measurements spanned over a period of one to two months, and we did not notice any change in permeability. For practical applications, this experiment should be run over years (or under accelerated conditions, such as at a higher temperature). More generally speaking, the stability of biaxially wrinkled films over time should be studied in details. Mechanical stability under cyclic stretch should also be studied.

We have created wrinkles by prestretching the substrate, attaching a flat foil, and then releasing the substrate. In the case of polyethylene wrinkles, concomitant buckling and delamination is observed. For aluminum wrinkles on a VHB substrate and deposited silica on PDMS, delamination is almost nonexistent. It is conceivable that one can create stretchable two-dimensional ordered wrinkles, such as Miura folding, by patterning the topography of the substrate or the film.[126,127] Deposition on a patterned soft substrate may enable stretchable seals without prestretching constraints. No matter which technique is used to prepare the wrinkles, adhesion to the substrate is of primary importance. A poor adhesion enables delamination of the foil, which can be harnessed to make large amplitude wrinkles and reach high stretchability. A poor adhesion can, however, lower the structure resilience due to interfacial fatigue cracks.

A plurality of designs and fabrication methods can be envisioned. Some of them will be compatible with roll-to-roll, digital fabrication, and dip-coating techniques. Designing stretchable seals is drawing attention toward new topics, such as the fatigue of wrinkles and the adhesion of a wrinkled film to a substrate. More generally speaking, biaxially wrinkled continuous thin films may serve new applications in stretchable electronics.

CONCLUSIONS

Long-time use of stretchable devices requires stretchable seals. At molecular level, stretchability and permeability are inextricably linked: soft and low-permeability materials do not exist. A scaling analysis shows that thin films of stiff, wrinkled, low-permeability materials can serve as stretchable seals. We have used polyethylene, aluminum, and silica films as low-permeability layers and elastomers as stretchable substrate. Wrinkled aluminum films are prone to fatigue fracture and cannot serve as stretchable seals. Wrinkled polyethylene and silica thin films demonstrate lower transmissibility than the bare elastomer and remain stretchable, and their transmissibility remains low after many cycles of stretching. We hope this work will stimulate the development of seals for stretchable devices.

MATERIALS

VHB (4905; 3M) was purchased from McMaster-Carr. Glad Press'N Seal food plastic wrap was used to make polyethylene/VHB laminates. Press'N Seal is a polyethylene thin film containing no plasticizer.[128] Reynolds Wrap heavy duty aluminum foil was used to make VHB/aluminum/VHB laminates. For poly(dimethylsiloxane) (Sylgard 184; Dow Corning), we used a 10:1 mixing ratio of precursor to curing agent. PDMS thin films were spin-coated onto the backside of plastic Petri

DOI: 10.1021/acsami.8b08910
ACS Appl. Mater. Interfaces XXXX, XXX, XXX−XXX

dishes of various diameters. A typical recipe to make a thin film about 200 μm thick consists of spinning at 300 rpm for 80 s. The PDMS films were cured overnight at 65 °C and then degassed for 12 h in a vacuum chamber. Silica was deposited by plasma-enhanced chemical vapor deposition (PECVD) using a Cirrus 150 machine from Nexx Systems. The substrate temperature was maintained below 140 °C (but is not exactly known) by helium backcooling. Deposition pressure was maintained at 10 mTorr, with a microwave power of 300 W. Silane and dioxygen flows were, respectively, maintained at 50 and 20 sccm during deposition. The growth rate is about 10.5 nm/min from previous calibrations on the same machine. The chamber can host samples as large as 5 in. in diameter. The maximum thickness of the sample inserted in the machine is about 1 cm, which allowed us to insert a homemade sample holder to apply a prestretch during deposition.

To measure the water transmissibility of the materials, we use exactly the same dry-cup setup fabricated for our previous work.[22] The thickness of each film (besides silica) was measured (using a Vernier scale, 10 μm precision). The thin films of Press'N Seal and aluminum were folded multiple times to measure the thickness more precisely. We measured the thickness of 20 samples of each material, and the values indicated the main text are "average value ±1 standard deviation". Absolute error bars for Figures 6 and 7 represent the standard deviation of the water transmissibility measurements. The water transmissibility was determined once a day based on mass variations of the cups for at least 7 days in a row. We study the stress−stretch behavior in uniaxial tension. A thin rectangular sheet (usually 50 × 60 × 0.5 mm^3) of the sample was fixed to rigid grips and mounted on a tensile tester (Instron model 5966) with a 500 N load cell. The strain rate was about 0.03 s^{-1} for the mechanical characterization in Figures 7, S5, and S6 and about 0.17 s^{-1} for the fatigue test in Figure S6.

Scanning electron microscopy images were taken using an Ultra-55 Field Emission Scanning Electron Microscope from Zeiss. The samples were first metallized by depositing a 5 nm thick layer of platinum/palladium using a HAR 050 EMS 300T D dual-head sputter coater.

■ ASSOCIATED CONTENT

Supporting Information

The Supporting Information is available free of charge on the ACS Publications website at DOI: 10.1021/acsami.8b08910.

Permeability of materials, stiffness−transmissibility trade-off for laminate and brick−mortar composites, analogy with the bending of an elastica, mechanical testing of polyethylene and aluminum wrinkles, model for the transmissibility of a wrinkled laminate, fatigue of wrinkled laminates in uniaxial tension (PDF)

■ AUTHOR INFORMATION

Corresponding Author

*E-mail: suo@seas.harvard.edu.

ORCID

Paul Le Floch: 0000-0001-7211-1699

Zhigang Suo: 0000-0002-4068-4844

Author Contributions

‖P.L.F. and S.H. contributed equally to this work.

Funding

The work at Harvard is supported by the NSF MRSEC (DMR-1420570). J.T. acknowledges the support of NSFC (No. 11702208) and the National Postdoctoral Program for Innovative Talents (No. BX201700192). J.L. was supported by China Scholarship Council as a visiting scholar for two years at Harvard University.

Notes

The authors declare no competing financial interest.

■ ACKNOWLEDGMENTS

This work was performed in part at the Center for Nanoscale Systems (CNS), a member of the National Nanotechnology Coordinated Infrastructure (NNCI), which is supported by the National Science Foundation under NSF award no. 1541959. CNS is part of Harvard University.

■ REFERENCES

(1) Robertson, G. L. *Food Packaging: Principle and Practices*, 3rd ed.; CRC Press, 2013.

(2) Chung, D. D. L. *Materials for Electronic Packaging*; Butterworth-Heinemann, 1995.

(3) Choi, M.-C.; Kim, Y.; Ha, C.-S. Polymers for Flexible Displays: From Material Selection to Device Applications. *Prog. Polym. Sci.* **2008**, *33*, 581−630.

(4) Haworth, J. P.; Baldwin, F. P. Butyl Rubber Properties and Compounding. *Ind. Eng. Chem.* **1942**, *34*, 1301−1308.

(5) Kim, D.-H.; Rogers, J. A. Stretchable Electronics: Materials Strategies and Devices. *Adv. Mater.* **2008**, *20*, 4887−4892.

(6) Rogers, J. A.; Someya, T.; Huang, Y. Materials and Mechanics for Stretchable Electronics. *Science* **2010**, *327*, 1603.

(7) Sekitani, T.; Someya, T. Stretchable, large-area Organic Electronics. *Adv. Mater.* **2010**, *22*, 2228−2246.

(8) Hammock, M. L.; Chortos, A.; Tee, B. C.; Tok, J. B.; Bao, Z. 25th anniversary article: The Evolution of Electronic Skin (e-skin): a brief history, design considerations, and recent progress. *Adv. Mater.* **2013**, *25*, 5997−6038.

(9) Chortos, A.; Liu, J.; Bao, Z. Pursuing Prosthetic Electronic Skin. *Nat. Mater.* **2016**, *15*, 937−950.

(10) Sekitani, T.; Noguchi, Y.; Hata, K.; Fukushima, T.; AIda, T.; Someya, T. A Rubberlike Stretchable Active Matrix Using Elastic Conductors. *Science* **2008**, *321*, 1468−1472.

(11) Shepherd, R. F.; Ilievski, F.; Choi, W.; Morin, S. A.; Stokes, A. A.; Mazzeo, A. D.; Chen, X.; Wang, M.; Whitesides, G. M. Multigait Soft Robot. *Proc. Natl. Acad. Sci. U.S.A.* **2011**, *108*, 20400−20403.

(12) Tolley, M. T.; Shepherd, R. F.; Mosadegh, B.; Galloway, K. C.; Wehner, M.; Karpelson, M.; Wood, R. J.; Whitesides, G. M. A Resilient, Untethered Soft Robot. *Soft Robotics* **2014**, *1*, 213−223.

(13) Wang, C.; Sim, K.; Chen, J.; Kim, H.; Rao, Z.; Li, Y.; Chen, W.; Song, J.; Verduzco, R.; Yu, C. Soft Ultrathin Electronics Innervated Adaptive Fully Soft Robots. *Adv. Mater.* **2018**, *30*, No. 1706695.

(14) Yang, C.; Suo, Z. Hydrogel Ionotronics. *Nat. Rev. Mater.* **2018**, *3*, 125−142.

(15) Kim, D. H.; Ghaffari, R.; Lu, N.; Rogers, J. A. Flexible and Stretchable Electronics for Biointegrated Devices. *Annu. Rev. Biomed. Eng.* **2012**, *14*, 113−28.

(16) Rogers, J. A.; Ghaffari, R.; Kim, D.-H. *Stretchable Bioelectronics for Medical Devices and Systems*; Springer, 2016; pp 1−317.

(17) Han, J.; Lee, J. Y.; Lee, J.; Yeo, J. S. Highly Stretchable and Reliable, Transparent and Conductive Entangled Graphene Mesh Networks. *Adv. Mater.* **2018**, *30*, No. 1704626.

(18) Dickey, M. D.; Chiechi, R. C.; Larsen, R. J.; Weiss, E. A.; Weitz, D. A.; Whitesides, G. M. Eutectic Gallium-Indium (EGaIn): A Liquid Metal Alloy for the Formation of Stable Structures in Microchannels at Room Temperature. *Adv. Funct. Mater.* **2008**, *18*, 1097−1104.

(19) Celle, C.; Cabos, A.; Fontecave, T.; Laguitton, B.; Benayad, A.; Guettaz, L.; Pélissier, N.; Nguyen, V. H.; Bellet, D.; Muñoz-Rojas, D.; Simonato, J.-P. Oxidation of Copper Nanowire based Transparent Electrodes in ambient Conditions and their Stabilization by Encapsulation: Application to Transparent Film Heaters. *Nanotechnology* **2018**, *29*, No. 085701.

(20) Wang, Y.; Zhu, C.; Pfattner, R.; Yan, H.; Jin, L.; Chen, S.; Molina-Lopez, F.; Lissel, F.; Liu, J.; Rabiah, N. I.; Chen, Z.; Chung, J. W.; Linder, C.; Toney, M. F.; Murmann, B.; Bao, Z. A highly Stretchable, Transparent, and Conductive Polymer. *Sci. Adv.* **2017**, *3*, No. e1602076.

DOI: 10.1021/acsami.8b08910
ACS Appl. Mater. Interfaces XXXX, XXX, XXX−XXX

(21) Kawano, K.; Pacios, R.; Poplavskyy, D.; Nelson, J.; Bradley, D. D. C.; Durrant, J. R. Degradation of Organic Solar Cells due to Air Exposure. *Sol. Energy Mater. Sol. Cells* **2006**, *90*, 3520−3530.
(22) Le Floch, P.; Yao, X.; Liu, Q.; Wang, Z.; Nian, G.; Sun, Y.; Jia, L.; Suo, Z. Wearable and Washable Conductors for Active Textiles. *ACS Appl. Mater. Interfaces* **2017**, *9*, 25542−25552.
(23) Lacour, S. P.; Jones, J.; Wagner, S.; Teng, L.; Zhigang, S. Stretchable Interconnects for Elastic Electronic Surfaces. *Proc. IEEE* **2005**, *93*, 1459−1467.
(24) Jones, J.; Lacour, S. P.; Wagner, S.; Suo, Z. Stretchable Wavy Metal Interconnects. *J. Vac. Sci. Technol. A* **2004**, *22*, 1723−1725.
(25) Song, J.; Jiang, H.; Liu, Z. J.; Khang, D. Y.; Huang, Y.; Rogers, J. A.; Lu, C.; Koh, C. G. Buckling of a Stiff Thin film on a Compliant Substrate in Large Deformation. *Int. J. Solids Struct.* **2008**, *45*, 3107−3121.
(26) Sun, Y.; Choi, W. M.; Jiang, H.; Huang, Y. Y.; Rogers, J. A. Controlled Buckling of Semiconductor Nanoribbons for Stretchable Electronics. *Nat. Nanotechnol.* **2006**, *1*, 201−207.
(27) Li, T.; Suo, Z.; Lacour, S. P.; Wagner, S. Compliant Thin film Patterns of Stiff Materials as Platforms for Stretchable Electronics. *J. Mater. Res.* **2005**, *20*, 3274−3277.
(28) Kim, D.-H.; Lu, N.; Ma, R.; Kim, Y.-S.; Kim, R.-K.; Wang, S.; Wu, J.; Won, S. M.; Tao, H.; Islam, A.; Yu, K. J.; Kim, T.-I.; Chowdhury, R.; ying, M.; Xu, Z.; Li, M.; Chung, H.-J.; Keum, H.; McCormick, M.; Liu, P.; Zhang, Y.-W.; Omenetto, F. G.; Huang, Y.; Coleman, T.; Rogers, J. A. Epidermal Electronics. *Science* **2011**, *333*, 838−843.
(29) Lipomi, D. J.; Tee, B. C.; Vosgueritchian, M.; Bao, Z. Stretchable Organic Solar Cells. *Adv. Mater.* **2011**, *23*, 1771−1775.
(30) Lipomi, D. J.; Bao, Z. Stretchable, Elastic Materials and Devices for Solar Energy Conversion. *Energy Environ. Sci.* **2011**, *4*, 3314.
(31) Oh, J.-Y.; Rondeau-Gagné, S.; Chortos, A.; Lissel, F.; Wang, G.-J.; Schroeder, B. C.; Kurosawa, T.; Lopez, J.; Katsumata, T.; Xu, J.; Zhu, C.; Gu, X.; Bae, W.-G.; Kim, Y.; Jin, L.; Chung, J. W.; Tok, J. B.-H.; Bao, Z.; et al. Intrinsically Stretchable and Healable Semiconducting Polymer for Organic Transistors. *Nature* **2016**, *539*, 411−415.
(32) Hong, S.; Lee, H.; Lee, J.; Kwon, J.; Han, S.; Suh, Y. D.; Cho, H.; Shin, J.; Yeo, J.; Ko, S. H. Highly Stretchable and Transparent Metal Nanowire Heater for Wearable Electronics Applications. *Adv. Mater.* **2015**, *27*, 4744−4751.
(33) Huang, G.-W.; Xiao, H.-M.; Fu, S.-Y. Wearable Electronics of Silver-Nanowire/Poly(dimethylsiloxane) Nanocomposite for Smart Clothing. *Sci. Rep.* **2015**, *5*, No. 13971.
(34) Han, S.; Hong, S.; Ham, J.; Yeo, J.; Lee, J.; Kang, B.; Lee, P.; Kwon, J.; Lee, S. S.; Yang, M. Y.; Ko, S. H. Fast Plasmonic Laser Nanowelding for a Cu-nanowire Percolation Network for Flexible Transparent Conductors and Stretchable Electronics. *Adv. Mater.* **2014**, *26*, 5808−5814.
(35) Xu, F.; Zhu, Y. Highly Conductive and Stretchable Silver Nanowire Conductors. *Adv. Mater.* **2012**, *24*, 5117−5122.
(36) Zang, J.; Ryu, S.; Pugno, N.; Wang, Q.; Tu, Q.; Buehler, M. J.; Zhao, X. Multifunctionality and Control of the Crumpling and Unfolding of Large-area Graphene. *Nat. Mater.* **2013**, *12*, 321−325.
(37) Compañ, V.; Andrio, A.; López-Alemany, A.; Riande, E.; Refojo, M. F. Oxygen Permeability of Hydrogel Contact Lenses with Organosilicon Moieties. *Biomaterials* **2002**, *23*, 2767−2772.
(38) Anseth, K. S.; Bowman, C. N.; Brannon-Peppas, L. Mechanical Properties of Hydrogels and their Experimental Determination. *Biomaterials* **1996**, *17*, 1647−1657.
(39) Lin, S.; Cao, C.; Wang, Q.; Gonzalez, M.; Dolbow, J. E.; Zhao, X. Design of Stiff, Tough and Stretchy Hydrogel Composites via Nanoscale Hybrid Crosslinking and Macroscale Fiber Reinforcement. *Soft Matter* **2014**, *10*, 7519−7527.
(40) Wise, D. L.; Houghton, G. The Diffusion Coefficient of ten slightly Soluble Gases in Water at 10−60 °C. *Chem. Eng. Sci.* **1966**, *21*, 999−1010.
(41) Carpenter, J. H. New Measurement of Oxygen Solubility in Pure and Natural Water. *Limnol. Oceanogr.* **1966**, *11*, 264.
(42) Tromans, D. Modeling Oxygen Solubility in Water and Electrolyte Solutions. *Ind. Eng. Chem. Res.* **2000**, *39*, 805−812.
(43) Agache, P. G.; Monneur, C.; Leveque, J. L.; De Rigal, J. Mechanical Properties and Young's Modulus of Human Skin in Vivo. *Arch. Dermatol. Res.* **1980**, *269*, 221−232.
(44) Scheuplein, R. J. *Handbook of Physiology, Reactions to Environmental Agents*; American Physiological Society, 1977, 299−322.
(45) Ashby, M. F. *Materials Selection in Mechanical Design*, 4th ed.; Elsevier, 2011.
(46) Materials Data Book (online handbook), http://www-mdp.eng.cam.ac.uk/web/library/enginfo/cueddatabooks/materials.pdf (accessed May 29, 2018).
(47) Helander, R. D.; Tolley, W. B. In Water Vapor Transmission Rate (WVTR) of Elastomeric Materials, Technology Vectors, 29th National SAMPE Symposium and Exhibition, MGM Grand Hotel, Reno, Nevada, April 3−5; MGM Grand Hotel, Reno, Nevada, 1984; pp 1373−1383.
(48) Wolff, E. G. *Introduction to the Dimensional Stability of Composite Materials*, 1st ed.; DEStech Publication, 2004.
(49) Van Amerongen, G. J. The Permeability of Different Rubbers to Gases and Its Relation to Diffusivity and Solubility. *J. Appl. Phys.* **1946**, *17*, 972−985.
(50) Van Amerongen, G. J. Influence of Structure of Elastomers on Their Permeability to Gases. *J. Polym. Sci.* **1949**, *5*, 307−332.
(51) Iyengar, Y. Relation of Water Vapor Permeability of Elastomers to Molecular Structure. *J. Polym. Sci., Part B: Polym. Lett.* **1965**, *3*, 663−669.
(52) Robeson, L. M. Polymer Membranes for Gas Separation. *Curr. Opin. Solid State Mater. Sci.* **1999**, *4*, 549−552.
(53) McKeen, L. W. *Permeability Properties of Plastics and Elastomers*, 3rd ed.; Matthew Deans Elsevier, 2012.
(54) Illinger, J. L.; Schneider, N. S.; Karasz, F. E. Water Vapor Transport in Hydrophilic Polyurethanes. *Permeability Plast. Films Coat.* **1974**, 183−196.
(55) VHB Tape Speciality Tapes 3M (online datasheet), https://multimedia.3m.com/mws/media/986695O/3m-vhb-tape-specialty-tapes.pdf (accessed May 29, 2018).
(56) Kamal, M. R.; Jinnah, I. A.; Utracki, L. A. Permeability of Oxygen and Water Vapor Through Polyethylene/Polyamide Films. *Polym. Eng. Sci.* **1984**, *24*, 1337−1347.
(57) Caballero, B.; Trugo, L.; Finglas, P. M. *Encyclopedia of Food Sciences and Nutrition*, 2nd ed.; Academic Press, 2003.
(58) Massey, L. K. *Permeability Properties of Plastics and Elastomers Plastics Design Library*; William Andrew Publishing, 2003.
(59) Lange, J.; Wyser, Y. Recent Innovations in Barrier Technologies for Plastic Packaging-a Review. *Packag. Technol. Sci.* **2003**, *16*, 149−158.
(60) Tsai, M.-H.; Tseng, I. H.; Liao, Y.-F.; Chiang, J.-C. Transparent Polyimide Nanocomposites with Improved Moisture Barrier using Graphene. *Polym. Int.* **2013**, *62*, 1302−1309.
(61) Jung, S.-Y.; Paik, K.-W. In Effects of Alignment of Graphene Flakes on Water Permeability of Graphene-epoxy Composite Film; Electronic Components & Technology Conference, IEEE 64th; IEEE: Orlando, FL, 2014.
(62) Huang, H.-D.; Ren, P.-G.; Chen, J.; Zhang, W.-Q.; Ji, X.; Li, Z.-M. High Barrier Graphene Oxide nanosheet/Poly(vinyl alcohol) Nanocomposite Films. *J. Membr. Sci.* **2012**, *409−410*, 156−163.
(63) Shorgen, R. Water Vapor Permeability of Biodegradable Polymers. *J. Environ. Polym. Degrad.* **1997**, *5*, 91−95.
(64) Parylene Properties (online datasheet), http://www.parylene.com/pdfs/PTC-Parylene_Properties_Chart.pdf (accessed may 29, 2018).
(65) Permeability of Teflon FEP Resins (online datasheet), http://www.goodyearrubberproducts.com/2012pdfs/O_rings_Catalog/files/assets/downloads/page0009.pdf (accessed May 29, 2018).
(66) Schweitzer, P. A. *Mechanical and Corrosion-Resistant Properties of Plastics and Elastomers*; Marcel Dekker, 2000.
(67) Matbase (online database. https://www.matbase.com/ (accessed March 17th).
(68) Matweb (online database). http://www.matweb.com/index.aspx (accessed March 17th).

DOI: 10.1021/acsami.8b08910
ACS Appl. Mater. Interfaces XXXX, XXX, XXX−XXX

(69) Visweswaran, B.; Mandlik, P.; Mohan, S. H.; Silvernail, J. A.; Ma, R.; Sturm, J. C.; Wagner, S. Diffusion of Water into Permeation Barrier Layers. *J. Vac. Sci. Technol., A* **2015**, *33*, No. 031513.
(70) Hanada, T.; Negishi, T.; Shiroishi, I.; Shiro, T. Plastic Substrate with Gas Barrier Layer and Transparent Conductive Oxide Thin Film for Flexible Displays. *Thin Solid Films* **2010**, *518*, 3089−3092.
(71) Wuu, D. S.; Lo, W. C.; Chiang, C. C.; Lin, H. B.; Chang, L. S.; Horng, R. H.; Huang, C. L.; Gao, Y. J. Plasma-Deposited Silicon Oxide Barrier Films on Polyethersulfone Substrates: Temperature and Thickness Effects. *Surf. Coat. Technol.* **2005**, *197*, 253−259.
(72) Itoh, Y.; Tadashi, N. Solubility and Diffusion Coefficient of Oxygen in Silicon. *Jpn. J. Appl. Phys.* **1985**, *24*, 279−284.
(73) Mikkelsen, J. R. The Diffusivity and Solubility of Oxygen in SIlicon. *MRS Proc.* **1985**, *59*, 19−30.
(74) Tsai, M.-H.; Wang, H.-Y.; Lu, H.-T.; Tseng, I.-H.; Lu, H.-H.; Huang, S.-L.; Yeh, J.-M. Properties of Polyimide/Al2O3 and Si3Ni4 Deposited Thin Films. *Thin Solid Films* **2011**, 4969−4973.
(75) Andringa, A. M.; Perrotta, A.; de Peuter, K.; Knoops, H. C.; Kessels, W. M.; Creatore, M. Low-Temperature Plasma-Assisted Atomic Layer Deposition of Silicon Nitride Moisture Permeation Barrier Layers. *ACS Appl. Mater. Interfaces* **2015**, *7*, 22525−22532.
(76) Dameron, A. A.; Davidson, D. D.; Burton, B. B.; Carcia, P. F.; McLean, R. S.; George, S. M. Gas Diffusion Barriers on Polymers Using Multilayers Fabricated by Al2O3 and Rapid SiO2 Atomic Layer Deposition. *J. Phys. Chem. C* **2008**, 4573−4580.
(77) Park, J.-S.; Chae, H.; Chung, H. K.; Lee, S. I. Thin Film Encapsulation for Flexible AM-OLED: a Review. *Semicond. Sci. Technol.* **2011**, *26*, No. 034001.
(78) Chatham, H. Oxygen Diffusion Barrier Properties of Transparent Oxide Coatings on Polymeric Substrates. *Surf. Coat. Technol.* **1994**, 1−9.
(79) AZoM (online database). https://www.azom.com/ (accessed March 17th).
(80) Seethamraju, S.; Kumar, S.; Madras, G.; Raghavan, S.; Ramamurthy, P. C.; et al. Million-Fold Decrease in Polymer Moisture Permeability by a Graphene Monolayer. *ACS Nano* **2016**, *10*, 6501−6509.
(81) Lee, C.; Wei, X.; Kysar, J. W.; Hone, J. Measurement of the Elastic Properties and Intrinsic Strength of Monolayer Graphene. *Science* **2008**, *321*, 385−388.
(82) Pierleoni, D.; Xia, Z. Y.; Christian, M.; Ligi, S.; Minelli, M.; Morandi, V.; Doghieri, F.; Palermo, V. Graphene-based Coatings on Polymer Films for Gas Barrier Applications. *Carbon* **2016**, *96*, 503−512.
(83) Viton A-401C Fluoroelastomers (online datasheet), https://www.chemours.com/Viton/en_US/assets/downloads/viton-a-401c-technical-information.pdf (accessed May 29, 2018).
(84) Peijs, T.; Van Vught, R.; Govaert, L. Mechanical Properties of Poly(vinyl Alcohol) Fibres and Composites. *Composites* **1995**, *26*, 83−90.
(85) Meyer, J.; Schmidt, H.; Kowalsky, W.; Riedl, T.; Kahn, A. The Origin of Low Water Vapor Transmission Rates Through Al2O3/ZrO2 Nanolaminates Gas-diffusion Barriers Grown by Atomic Layer Deposition. *Appl. Phys. Lett.* **2010**, *96*, No. 243308.
(86) Dollinger, F.; Nehm, F.; Müller-Meskamp, L.; Leo, K. Laminated Aluminum Thin-Films as Low-Cost Opaque Moisture Ultra-Barriers for Flexible Organic Electronic Devices. *Org. Electron.* **2017**, *46*, 242−246.
(87) Rogers, C. E. Permeability and Chemical Resistance. In *Engineering Design for Plastics*; Baer, E., Ed.; Van Nostrand-Reinhold: Princeton, 1964.
(88) Norton, F. J. Permeation of Gaseous Oxygen through Vitreous Silica. *Nature* **1961**, *191*, 701.
(89) Jamieson, E. H. H.; Windle, A. H. Structure and Oxygen-Barrier Properties of Metallized Polymer Film. *J. Mater. Sci.* **1983**, *18*, 64−80.
(90) Leterrier, Y. Durability of Nanosized Oxygen-Barrier Coatings on Polymers. *Prog. Mater. Sci.* **2003**, *48*, 1−55.
(91) Miller, K. S.; Krochta, J. M. Oxygen and Aroma Barrier Properties of Edible Films: A Review. *Trends Food Sci. Technol.* **1997**, *8*, 228−237.
(92) Ryder, L. Oxygen-Barrier Containers-their Design and Cost. *Plast. Eng.* **1984**, *40*, 41−48.
(93) Brandrup, J.; Immergut, E. H.; Grulke, E. A.; Abe, A.; Bloch, D. R. *Polymer Handbook*; Wiley: New York, 1989; Vol. *7*.
(94) Tropsha, Y. G.; Harvey, N. G. Activated Rate Theory Treatment of Oxygen and Water Transport through Silicon Oxide/ Poly(ethylene terephthalate) Composite Barrier Structures. *J. Phys. Chem. B* **1997**, *101*, 2259−2266.
(95) Czeremuszkin, G. K.-S.; J.E.Wertheimer, M. R. Transparent Barrier Coatings on Polyethylene Terephthalate by Single- and Dual-Frequency Plasma-Enhanced Chemical Vapor Deposition. *J. Vac. Sci. Technol., A* **1998**, *16*, 3190−3198.
(96) Slee, J. A.; Orchard, G. A. J.; Bower, D. I.; Ward, I. M. The Transport of Oxygen Through Oriented Poly(ethylene terephthalate). *J. Polym. Sci., Part B: Polym. Phys.* **1989**, *27*, 71−83.
(97) Hernandez, R. J. Effect of Water Vapor on the Transport Properties of Oxygen through Polyamide Packaging Materials. *Water in Foods*; Pergamon: Amsterdam, 1994; pp 495−507.
(98) Mandlik, P. *A Novel Hybrid Inorganic-Organic Single Layer Barrier for Organic Light-Emitting Diodes*; Princeton University, 2009.
(99) Roberts, A. P.; Henry, B. M.; Sutton, A. P.; Grovenor, C. R. M.; Briggs, G. A. D.; Miyamoto, T.; Kano, M.; Tsukahara, Y.; Yanaka, M. Gas Permeation in Silicon-Oxide/Polymer (SiOx/PET) Barrier Films: Role of the Oxide Lattice, Nano-Defects and Macro-Defects. *J. Membr. Sci.* **2002**, *208*, 75−88.
(100) Yanaka, M.; Henry, B. M.; Roberts, A. P.; Grovenor, C. R. M.; Briggs, G. A. D.; Sutton, A. P.; Miyamoto, T.; Tsukahara, Y.; Takeda, N.; Chater, R. J. How Cracks in SiOx-Coated Polyester Films affect Gas Permeation. *Thin Solid Films* **2001**, *397*, 176−185.
(101) Tropsha, Y. G.; Harvey, N. G. Activated Rate Theory Treatment of Oxygen and Water Transport through Silicon Oxide/ Poly(ethylene terephthalate) Composite Barrier Structures. *J. Phys. Chem. B* **1997**, *101*, 2259−2266.
(102) Vohra, A.; Filiatrault, H. L.; Amyotte, S. D.; Carmichael, R. S.; Suhan, N. D.; Siegers, C.; Ferrari, L.; Davidson, G. J. E.; Carmichael, T. B. Reinventing Butyl Rubber for Stretchable Electronics. *Adv. Funct. Mater.* **2016**, *26*, 5222−5229.
(103) Vohra, A.; Carmichael, R. S.; Carmichael, T. B. Developing the Surface Chemistry of Transparent Butyl Rubber for Impermeable Stretchable Electronics. *Langmuir* **2016**, *32*, 10206−10212.
(104) Hauch, J. A.; Schilinsky, P.; Choulis, S. A.; Rajoelson, S.; Brabec, C. J. The Impact of Water Vapor Transmission Rate on the Lifetime of Flexible Polymer Solar Cells. *Appl. Phys. Lett.* **2008**, *93*, No. 103306.
(105) Garner, S.; Glaesemann, S.; Li, X. Ultra-slim Flexible Glass for Roll-to-Roll Electronic Device Fabrication. *Appl. Phys. A* **2014**, *116*, 403−407.
(106) Nielsen, L. E. Models for the Permeability of Filled Polymer Systems. *J. Macromol. Sci., Part A: Pure Appl.Chem.* **1967**, *1*, 929−942.
(107) Bharadwaj, R. K. Modeling the Barrier Properties of Polymer-Layered Silicate Nanocomposites. *Macromolecules* **2001**, *34*, 9189−9192.
(108) Cui, Y.; Kundalwal, S. I.; Kumar, S. Gas Barrier Performance of Graphene/Polymer Nanocomposites. *Carbon* **2016**, *98*, 313−333.
(109) Suo, Z.; Ma, E. Y.; Gleskova, H.; Wagner, S. Mechanics of Rollable and Foldable Film-on-Foil Electronics. *Appl. Phys. Lett.* **1999**, *74*, 1177−1179.
(110) Sharpe, W. N.; Pulskamp, J.; Gianola, D. S.; Eberl, C.; Polcawich, R. G.; Thompson, R. J. Strain Measurements of Silicon Dioxide Microspecimens by Digital Imaging Processing. *Exp. Mech.* **2007**, *47*, 649−658.
(111) Wiederhorn, S. M.; Fields, B. A.; Hockey, B. J. Fracture of Silicon Nitride and Silicon Carbide at Elevated Temperatures. *Mater. Sci. Eng. A* **1994**, *176*, 51−60.
(112) Euler, L. *Methodus Inveniendi Lineas Curvas Maximi Minimive Proprietate Gaudentes Sive Solutio Problematis Isoperimetrici Latissimo Sensu Accepti*; Springer Science & Business Media, 1952.
(113) Love, A. E. H. *A Treatise on The Mathematical Theory of Elastivity*; Cambridge University Press, 1892.

DOI: 10.1021/acsami.8b08910
ACS Appl. Mater. Interfaces XXXX, XXX, XXX−XXX

(114) Antman, S. S. *Nonlinear Problems of Elasticity*, 2nd ed.; Springer, 2005; Vol. *107*.
(115) Pacheco, M. E.; Piña, E. The Elastic Rod. *Revista mexicana de física E* **2007**, *53*, 186−190.
(116) Audoly, B.; Pomeau, Y. *Elasticity and Geometry*; Oxford University Press, 2010.
(117) Moon, M. W.; Lee, K. R.; Oh, K. H.; Hutchinson, J. W. Buckle Delamination on Patterned Substrates. *Acta Mater.* **2004**, *52*, 3151−3159.
(118) Mei, H.; Landis, C. M.; Huang, R. Concomitant Wrinkling and Buckle-Delamination of Elastic Thin Films on Compliant Substrates. *Mech. Mater.* **2011**, *43*, 627−642.
(119) Bowden, N.; Brittain, S.; Evans, A. G.; Hutchinson, J. W.; Whitesides, G. M. Spontaneous Formation of Ordered Structures in Thin Films of Metals Supported on an Elastomeric Polymer. *Nature* **1998**, *393*, 146−149.
(120) Chen, X.; Hutchinson, J. W. Herringbone Buckling Patterns of Compressed Thin Films on Compliant Substrates. *J. Appl. Mech.* **2004**, *71*, 597.
(121) BIPM, I.; IFCC, I.; IUPAC, I.; ISO, O., Evaluation of Measurement Data—Guide to the Expression of Uncertainty in Measurement, JCGM 100: 2008 *Citado en las* 2008, 167.
(122) Huang, Z.; Hong, W.; Suo, Z. Evolution of Wrinkles in Hard Films on Soft Substrates. *Phys. Rev. E* **2004**, *70*, No. 030601.
(123) Breid, D.; Crosby, A. J. Effect of Stress State on Wrinkle Morphology. *Soft Matter* **2011**, *7*, 4490.
(124) Li, B.; Cao, Y.-P.; Feng, X.-Q.; Gao, H. Mechanics of Morphological Instabilities and Surface Wrinkling in Soft Materials: a Review. *Soft Matter* **2012**, *8*, 5728.
(125) Cai, S.; Breid, D.; Crosby, A. J.; Suo, Z.; Hutchinson, J. W. Periodic Patterns and Energy States of Buckled Films on Compliant Substrates. *J. Mech. Phys. Solids* **2011**, *59*, 1094−1114.
(126) Song, Z.; Ma, T.; Tang, R.; Cheng, Q.; Wang, X.; Krishnaraju, D.; Panat, R.; Chan, C. K.; Yu, H.; Jiang, H. Origami Lithium-Ion Batteries. *Nat. Commun.* **2014**, *5*, No. 3140.
(127) Miura, K. *Method of Packaging and Deployment of Large Membranes in Space*; The Institute of Space and Astronautical Science Report, 1985.
(128) Glad Products FAQs. https://www.glad.com/faq/ (accessed March 17th).

DOI: 10.1021/acsami.8b08910
ACS Appl. Mater. Interfaces XXXX, XXX, XXX−XXX